25th ABCM International Congress of Mechanical Engineering
October 20-25, 2019, Uberlândia, MG, Brazil

COB-2019-0623
EFFECT OF IMPERFECT FIBER/MATRIX INTERPHASE: A MICROMECHANICAL MODEL FOR PREDICTING LONGITUDINAL AND SHEAR FAILURE IN COMPOSITE MATERIALS

José Humberto S. Almeida Jr.[1]
[1]Mechanics and Composite Materials Department, Leibniz-Institut für Polymerforschung, Hohe Straße 6, 01069 Dresden, Germany.
humberto@ipfdd.de; bittrich-lars@ipfdd.de; spickenheuer@ipfdd.de

Maísa Milanez Ávila Dias Maciel[2]
Volnei Tita[2]
[2]Department of Aeronautical Engineering, São Carlos School of Engineering, University of São Paulo, Av. João Dagnone, 1100, 13573-120 São Carlos, SP.
maisa.madm@usp.br; voltita@sc.usp.br

Abstract. *The macroscopic properties of carbon fiber-reinforced polymer composites (CFRP) depend upon the properties, the interfacial bonding conditions of the constituent phases (fiber and matrix), and the microstructure of the composites. In this research, a numerical methodology to model non-perfect interphase for thin interphase is presented. A transversely isotropic representative volume element (RVE) with circular fibers embedded into a square bulk polymer matrix was developed in order to calculate the effective coefficients of the constitutive tensor for several imperfect contact conditions. The effective coefficients were successfully calculated by using dummy values of shear interphase modulus in order to illustrate the variation of the effective coefficients in case of imperfect interphase. After this step, the material properties and stress-strain curves were predicted for composite materials. In addition, those results can be used as input in a macro-scale model to predict the mechanical response of a composite structure considering imperfect fiber-matrix interphase. The results showed that for a longitudinal loading the interphase does not influence the composites mechanical response, however, it plays a critical role when the shear loading is applied.*

Keywords: *Fiber-matrix interphase, micromechanical modeling, failure of composite materials.*

1. INTRODUCTION

CFRPs are well known as hierarchical materials with three structural levels: micro-scale, intermediate and macro-scale. The micro-scale defines the arrangement of fibers in the composite; the intermediate level generally relates to the lamina geometry, and the macro-scale refers to the global structural response of the material. In a multi-scale framework of CFRP simulation, the micro-scale approaches are usually applied to predict the effective stiffness and strength properties of transversely isotropic constitutive properties of composites, which then serves as theoretical tools for engineering structure design (Wang et al., 2016). Failure mechanisms of CFRPs still are a challenging issue, mainly because of the anisotropic nature of the carbon fiber, which complicates the numerical modeling. Unidirectional (UD) CFRPs subjected to transverse tensile loads often fail by two different failure mechanisms: one is the matrix damage and the other is micro-cracks at the fiber/matrix interphase. For longitudinal loading, matrix and fiber cracking are the most often seen failure modes (Vajari et al., 2013).

Yang et al., (2012) developed a micromechanical damage model considering random fiber distribution in order to reveal the failure mechanisms of UD CFRP composites under transverse tension and compression. It was concluded that the tensile failure initiated as interfacial debonding then it evolves as a result of interactions between interfacial debonding and matrix plastic deformation, while the compressive failure was dominated by plastic matrix damage. Totry et al., (2010) studied the effect of fiber, matrix and interphase properties on the in-plane shear response of CFRP laminates experimentally and numerically. It was found that in-plane shear behavior of cross-ply laminates was controlled by the matrix yield strength and the interphase strength was independent of the fiber properties.

There are numerous works dealing with micromechanical modeling of composite laminates under transverse loads. For simplification purposes, in longitudinal loads, the maximum stress criterion is often used, however, local or partial debonding of the fiber/matrix interphase might play a key role (Shari et al., 1995). For instance, when a UD laminate is under longitudinal tension the splitting of some bundles, fiber pull-out or imperfect fiber/matrix contact can be accounted for some of the non-linearity throughout in the loading history. The interphase is a transition zone between the fiber (first phase) and the matrix (second phase). This third phase may result from the manufacturing process for most fiber-reinforced composites. Although the thickness of the interphase is very small, this third phase plays a vital role in the reliability of CFRPs and affects their global mechanical response considerably. For instance, if the fiber/matrix adhesion is imperfect, then the continuity conditions for stresses and displacements are not satisfied (Tita et al., 2015).

In this context, this investigation proposes a micromechanical model to predict the material properties and stress-strain curves for composite materials considering different degrees of fiber/matrix imperfection. For that, first, the micromechanical model is developed in order to determine the effective coefficients of the constitutive matrix. A reverse methodology is proposed, in which an energy-based method is used, where the energy from the experimental curves of a real specimen is calculated and used to find the required load (l) to generate the experimental response based on the energy from any particular point throughout the stress-strain curve.

2. MATERIALS AND METHODOLOGY

2.1 Materials and testing

The main focus of this work is the micromechanical model, therefore the experimental data used here was available at the research group, however a brief description of the materials and the testing procedures is given in this topic. The material used was a Hexcel M9/M10 prepreg, which was hand laminated and autoclave cured by 120 °C, with pressure between 0,3 and 5 bar for 60 min. The specimen with fiber orientation at 0° had 5 layers and its configuration was according the ASTM D3039, 250 mm x 15 mm x 0,9 mm (Length x Width x Thickness). The specimen with fiber orientation at +/-45° had 8 layers and was symmetric, its configuration was according the ASTM D3518, 250 mm x 25 mm x 2,7 mm (Length x Width x Thickness) (Tita et al., 2015).

The tensile test was carried out according the ASTM D3039/D3039M-95a for the specimen with fibers at 0°, and the test velocity was 1 mm/min.

The shear response of the material was carried out according the ASTM D3518. This test method determines the in-plane shear response of polymer matrix composite materials with fibers at +/-45°. Therefore, for the material coordinate system, the specimens are tested under shear. Test velocity was 2 mm/min

2.2 Micromechanical Modeling

The aim of this work is to develop a micromechanical model to predict both the linear and non-linear part of the stress-strain curve of composite materials. In micromechanical models, the individual properties of the constituent materials (fiber and matrix), and composites configuration such as fiber geometry, fiber volume fraction, and imperfect contact, are taken into consideration. The hypothesis used is that the non-linearity at the end of the stress-strain curve can be attributed to the beginning of the degradation process of fiber-matrix interphase In this work, the shear interface modulus will be considered as a measure of interphase quality. Therefore, the only accounted failure method described in this model is of interphase failure.

For that, firstly, a representative volume element (RVE) is generated via Python script and analyzed numerically via finite element (FE) analysis in Abaqus package. In this case, a square fiber arrangement is chosen: the RVE is a 1 mm^3 cube, and the fiber is a central cylinder, as shown in Figure 1. The fiber volume fraction (Vf) used is 62%. In addition, a thin layer is added at the boundary between the fiber and the matrix to represent the interphase. Based on Tita et al., 2015. The interphase volume fraction (If) must be determined based on a relation of interphase thickness and the fiber radius, which leads to an I_f of 0.12%.

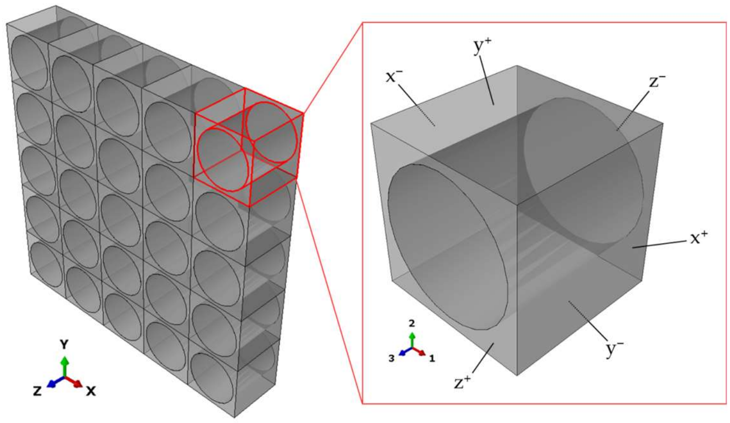

Figure 1. Periodic FRPC with circular fibers embedded into a square bulk matrix (left) highlighting a unit cell (right).

The next step is to define the material properties separately. Each element (fiber, matrix, and interphase) is considered as being isotropic and homogenous. Particularly in the case of the interphase, the shear modulus (G_i) is a parameter related to the fiber/matrix contact. For high G values, the contact is perfect, so the stress is transferred from the matrix to the fiber. The higher the G_i , the greater the interfacial contact. When G_i reaches very small values (i.e. 1), there is no fiber/matrix contact anymore. The idea is then to vary the G_i values (that physically represents the transition from a perfect interphase to a non-perfect one) in order to understand how it will affect the CFRP properties. Essentially, the model looks to incorporate the fiber/matrix adhesion characteristics obtained into a progressive damage model. At the end, a macro model will be able to incorporate and consider the fiber/matrix interphase behavior in the analysis.

The constitutive equation of the composites studied can be written in the matrix form as Eq. (1) For a transversally isotropic composite laminate, where σ_{ij} and ε_{kl} are the stress and infinitesimal strain tensors, where the contracted Voigt notation is used.

$$\begin{Bmatrix} \sigma_{11} \\ \sigma_{22} \\ \sigma_{33} \\ \sigma_{23} \\ \sigma_{13} \\ \sigma_{12} \end{Bmatrix} = \begin{bmatrix} C_{11} & C_{12} & C_{13} & 0 & 0 & 0 \\ C_{12} & C_{11} & C_{13} & 0 & 0 & 0 \\ C_{13} & C_{13} & C_{33} & 0 & 0 & 0 \\ 0 & 0 & 0 & C_{44} & 0 & 0 \\ 0 & 0 & 0 & 0 & C_{44} & 0 \\ 0 & 0 & 0 & 0 & 0 & C_{66} \end{bmatrix} \begin{Bmatrix} \varepsilon_{11} \\ \varepsilon_{22} \\ \varepsilon_{33} \\ \varepsilon_{23} \\ \varepsilon_{13} \\ \varepsilon_{12} \end{Bmatrix} \tag{1}$$

The homogenization approach for composite materials relies on finding dependence between the average variables of the material model, which may represent coherent physical behavior (Brito-Santana et al., 2016). Based on the theorem of average, the mechanical properties of the RVE are taken from the average properties of the composite laminate. It is assumed that the average mechanical properties of an RVE are equal to the average properties of the composite laminate, as Eq. (2). Where $\langle T_{ij} \rangle$ is the second rank stress tensor and $\overline{T_{ij}}$ is the average stress. In this case, the average stress in the RVE is defined by Eq. (3), where $|V|$ is the RVE volume, and using FE analysis, the average results can be calculated Eq. (4)., where nel is the number of elements of the RVE, $T_{ij}^{(n)}$ and $V^{(n)}$ are the evaluated tensor and volume of the nth element.

$$\langle T_{ij} \rangle = \overline{T_{ij}} \tag{2}$$

$$\overline{T_{ij}} = \frac{1}{|V|} \int_{|V} T_{ij}^{0} dV \tag{3}$$

$$\overline{T_{ij}} = \frac{1}{|V|} \sum_{n=1}^{nel} T_{ij}^{(n)} V^{(n)} \tag{4}$$

For a complete description to determine effective material properties, it is necessary to formulate suitable boundary conditions (BCs). Figure1 presents a periodic CFRP structure with a square arrangement and a circular fiber embedded into a bulk polymer matrix, and the fiber is aligned with the z-axis (direction 3). A 3D model with fiber and matrix meshed with an eight-node linear brick element with reduced integration and hour glass control (C3D8R) is developed.

The set of constitutive equations in the matrix (Eq. (1)), with prescribed boundary conditions, allow the evaluation of the effective material properties. For a given particular BCs applied in the RVE, more than one coefficient is obtained for each analysis. Therefore, to calculate all 6 effective coefficients, only 4 analyses are required. Table 1 presents a summary of the loads and BCs used.

Table 1. Loadings and boundary conditions (BCs) for calculating all effective coefficients

Equation	***Displacement field (m)***	***Loading field (N)***	***Displacement BCs (m)***
$c_{11}^{eff} = \frac{\overline{T}_{11}}{\overline{\varepsilon}_{11}}$ & $c_{12}^{eff} = \frac{\overline{T}_{22}}{\overline{\varepsilon}_{11}}$	Positive u_x: face x^+	---	$\varepsilon_{22} = \varepsilon_{33} = \varepsilon_{12} = \varepsilon_{23} = \varepsilon_{13} = 0$
$c_{13}^{eff} = \frac{\overline{T}_{11}}{\overline{\varepsilon}_{33}}$ & $c_{33}^{eff} = \frac{\overline{T}_{33}}{\overline{\varepsilon}_{33}}$	Positive u_z: face z^+	---	$\varepsilon_{11} = \varepsilon_{22} = \varepsilon_{12} = \varepsilon_{23} = \varepsilon_{13} = 0$
$c_{66}^{eff} = \frac{\overline{T}_{12}}{\overline{\varepsilon}_{12}}$	---	$+F_y$ & $-F_y$ at faces x^+ & x^- $+F_x$ & $-F_x$ at faces y^+ & y^-	$u_y = 0, at\ x^+x^-\ and\ u_x = 0, at\ y^-$ Uniform x-displacement at the face: y^+
$c_{44}^{eff} = \frac{\overline{T}_{23}}{\overline{\varepsilon}_{23}}$	---	$+F_y$ & $-F_y$ at faces z^+ & z^- $+F_z$ & $-F_z$ at faces y^+ & y^-	$u_y = 0, at\ z^+z^-\ and\ u_z = 0, at\ y^-$ Uniform z-displacement at the face: y^+

In order to predict the material properties and stress-strain curves of composite materials, a reverse methodology is herein proposed. The whole methodology is hereafter described, as follows:

i. Develop the RVE and apply adequate BCs for calculating specific effective coefficients;
ii. Calculate the effective coefficients with Python scripts in Abaqus FE package and collect the stress and strain tensors numerically;
iii. For a given laminate under experimental test (from Tita, 2003), calculate the energy at each point of the σ *vs.* ε curve, i.e. the area below de curve;
iv. Impose strain on the RVE (microscale) and calculate stress on the RVE for the same energy calculated in iii, and by using the theorem of average, inverse analyses and optimize the process to compute G_i for that energy level;
v. The obtained relationship between G_i and imposed local strain will allow knowing the degree of fiber/matrix adhesion imperfection for each point;
vi. A relationship between a calibrated value of the effective coefficients *vs.* $\bar{G}$ $(G_i + G_f)$ can be established by using different values for the degree of imperfections in the interphase of the RVE;
vii. Based on the relation between G_i and imposed local strain, it is possible to determine G_i for a given strain level. Then, based on the relationship between the effective coefficients *vs.* $\bar{G}$ $(G_i + G_f)$, it is possible to calculate degraded material properties. Thus, these degraded properties are used to predict stress-strain curves;
viii. Finally, an efficient and fast degradation methodology can be applied into a macro model in order to predict the response of a composite structure, considering interphase imperfections.

The methodology is summarized in Figure 2.

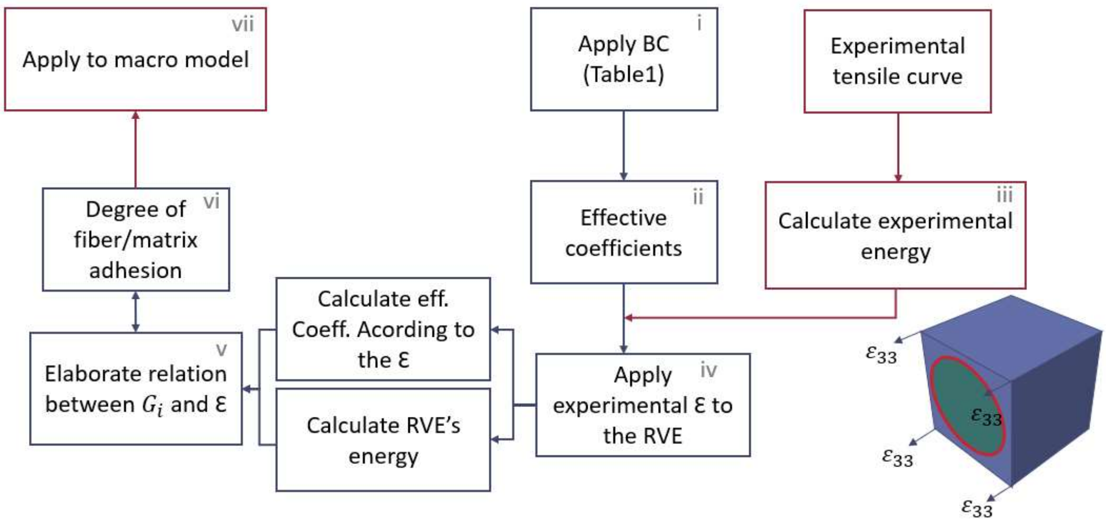

Figure 2. Methodology schematic diagram

3. RESULTS

3.1 Determination of Effective Coefficients

Following the methodology previously described, the step ii) was made, and the effective coefficients were calculated after applying the suitable loading and BCs, coefficients $c_{11}^{eff}, c_{12}^{eff}, c_{13}^{eff}, c_{33}^{eff}$, and c_{44}^{eff} are shown in Figure 2.

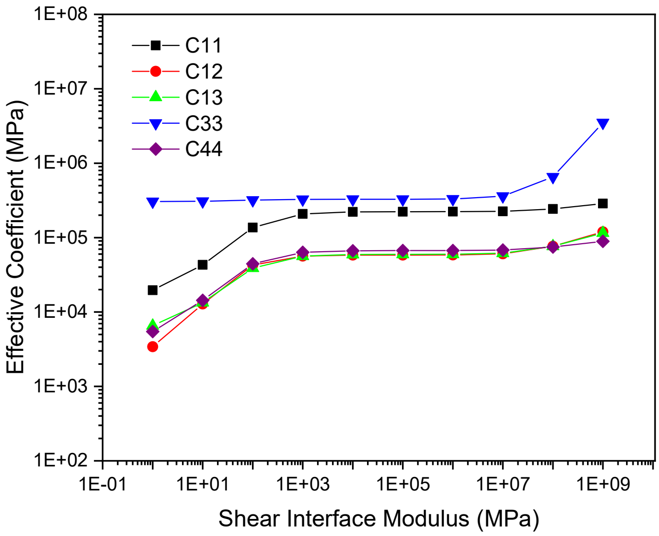

Figure 3. Variation of three effective coefficients with the shear interphase modulus ($\boldsymbol{G_i}$).

In this work, the shear interphase modulus (G_i) was used as an indicator of interphase condition, thus a very high G_i (100 GPa) indicated the perfect fiber-matrix interphase. In order to show the importance of the interphase condition in the material's final longitudinal or shear mechanical properties, the effective coefficients were calculated by different values of G_i, which varied from perfect contact to no contact. Figure 3 shows that by increasing G_i, all of the calculated effective coefficients increase in value. According to Fig.3, the C_{33}, does not vary when the interphase properties are increased. however, for very high G_i. values, which could indicate a perfect fiber/matrix adhesion configuration, an increase in the value of the C_{33} coefficient is observed. This behavior can be explained by the fact that, since fiber modulus values are much higher than either matrix or interphase, it becomes the main load bearing component. As for the other coefficients, the C_{11} shows a decrease for very low G_i values, indicating that tensile perpendicular to the fiber would only be affected for a fully debonded configuration. For the C_{12} and C_{13}, a similar behavior is observed, however, both of them shows an increase when higher values of G_i are observed.

For the step iii), experimental data was used for the calculations of the material overall modulus and the energy. Table 2 shows the experimental data of the material stress-strain curve, the points 1-8 represent stages of the experimental stress-strain curve which will be used as marks for the finite element model, these experimental points can also be observed at Fig.4 and Fig.5.

Table 2. Experimental stress-strain data obtained by two different with fibers at 0° and at +/- 45°

Orientation	**0°**		
Point	**Strain (%)**	**Stress (MPa)**	**Updated Modulus (1) (GPa)**
1	0,20	250	125,00
2	0,38	500	131,58
3	0,65	750	115,92
4	0,90	1000	111,11
5	1,20	1250	104,17
6	1,50	1500	100,00
7	2,00	1750	87,50
8	2,50	2000	80,00
Orientation	**+/- 45°**		
Point	**Strain (%)**	**Stress (MPa)**	**Updated Modulus (1) (GPa)**
1	0,29	15	5,10
2	0,40	20	4,96
3	0,52	25	4,78
4	0,66	30	4,57
5	0,81	35	4,31
6	1,00	40	4,00
7	1,25	45	3,60
8	1,68	50	2,98

(1) Angular coefficient between previous and current point

3.2 Prediction of stress-strain curves

Following the steps proposed in item 2, step v. is to develop a model in order to verify the fit o the linear portion of the stress-strain curve. Figure 4 shows the stress-strain curve for points 1 through 8 for the experimental data shown in Tab.2 and the modeled stress-strain curve.

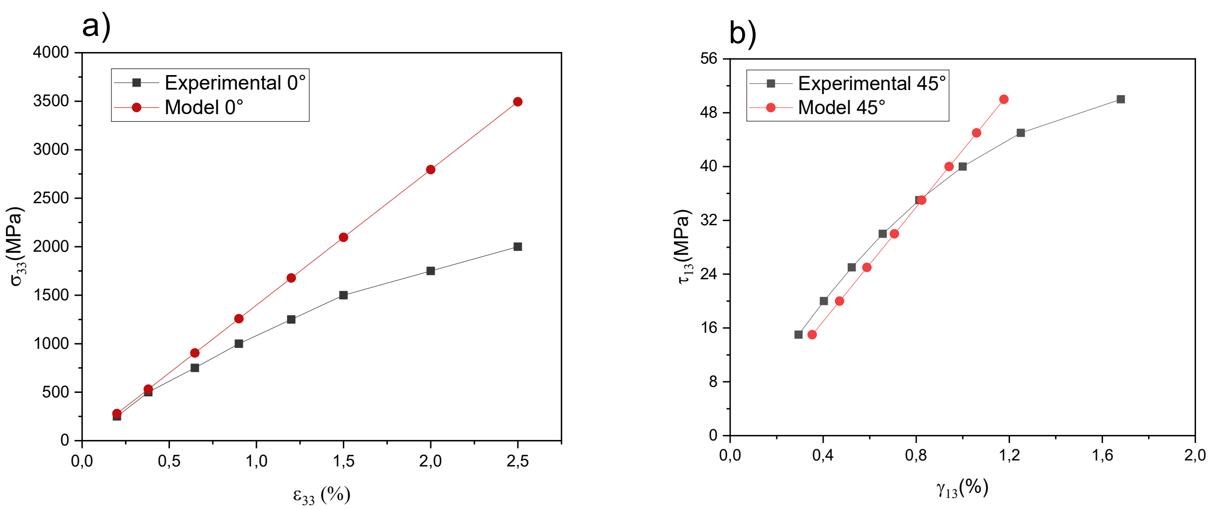

Figure 4. Preliminary model stress-strain curve, in red, and experimental curve, in black, for two different fiber orientations, a) fibers at 0° and for b) fibers at +/-45°

Figure 4 shows the stress-strain curve for the experimental data shown in Tab.2 and the modeled stress-strain curve. For the curve a) the fit was well until point 2, from this point onwards they both start to diverge, exceeding a difference of approximately 56% at point 8. However, the model was shown to agree well in the linear part. Figure 4 b) shows that the initial portion of the curve has a slightly lower inclination, thus a smaller shear modulus. However, at point 5 the shear modulus approximates to the experimental data, and due to its linearity, it continues to diverge from the experimental data.

The next step after the linear model is to develop a model that can account for the nonlinear part of the mechanical response by the degradation of the interphase property. Figure 5 shows the modeled response for the degraded interphase properties.

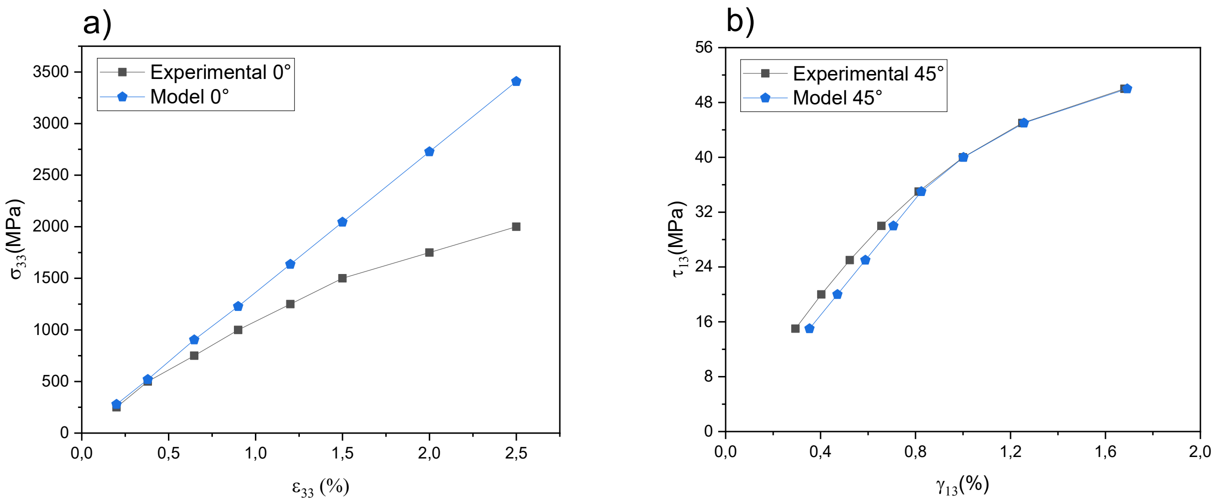

Figure 5. A model accounting for interphase degradation stress-strain curve for two different fiber orientations, a) fibers at 0° and for b) fibers at +/-45°..

Figure 5 a) shows that for the modeled response at 0° the degraded interphase properties have little influence on the overall RVE final properties, thus showing a very similar graphic to Fig 4. This is understandable since at 0° the main final properties are the fiber elastic modulus, and since no degradation step was added to then, the overall properties remained the same (Swolfs et al., 2016). In other words, for this case, the response is driven by fiber failure no interface imperfections.

As for the shear test with fiber at +/-45°, shown in Fig. 5 b), the degradation of the interphase properties has greatly impacted on the nonlinear part of the curve. Therefore, for the shear stress, the interphase accounted for a great part of the RVE's overall mechanical response. This happens because, even though the fiber accounts for the material's strength, the matrix and interphase have to evenly distribute the stress across the composite. Therefore, when the interphase is degraded the stress is not distributed to the fiber, which leads to a decrease in the material's overall stiffness (Tita et al., 2015).

4. CONCLUSIONS

This paper shows a micromechanical model using a RVE and a methodology for predicting composite materials response, considering interface imperfections. First, by the use of the RVE, the effective coefficients were calculated in regards to an imperfect interphase. It was observed that in regards to C_{33}, the value of the coefficients decreased with the decreasing of the interphase values until the Gi reached very high values of interphase properties, therefore a perfect was considered. Then the C_{33eff} values stabilized, which was attributed to the fact that in the fiber direction, 0°, the fiber is the main component responsible for the RVE's overall mechanical response. This can be confirmed when, by modeling the degradation step the inclination of the stress-strain curve did not change even after fully degraded interphase properties were used. As for the composites shear properties (fiber at +/-45°), the model was successful in accounting for the nonlinear part of the curve. Thus, the interphase degrading model was shown to be successful for the shear stress, however, for the 0° loading the model suggests that fiber degrading must be added for future models. In addition, this efficient and fast degradation methodology can be applied into a macro model in order to predict the response of a composite structure, considering interphase imperfections.

5. ACKNOWLEDGMENTS

J.H.S. Almeida Jr. Is grateful for CAPES and Alexander von Humboldt for the financial support; V. Tita is thankful to National Council for Scientific and Technological Development (CNPq process number: 428591/2016-7 and

310656/2018-4). Maisa M. A. D. Maciel is thankful for CAPES (PROAP funding). This study was financed in part by the Coordenação de Aperfeiçoamento de Pessoal de Nível Superior - Brasil (CAPES) Finance Code 001.

6. REFERENCES

Brito-Santana, H., Medeiros, R., Rodriguez-Ramos, R., Tita, V., 2016, "Different interphase models for calculating the effective properties in piezoelectric composite materials with imperfect fiber-matrix adhesion", *Composite Structures*, Vol. 151, pp. 70-80.

Shari H.Z. and Chou T.W., 1995 "Transverse elastic moduli of unidirectional fiber composite with fiber/matrix interfacial debonding", *Composites Science and Technology*, Vol. 53, pp. 383–391.

Tita, V., 2003, "Contribuição ao estudo de danos e falhas progressivas em estruturas de material compósito polimérico", Tese (Doutorado) – Escola de Engenharia de São Carlos, Universidade de São Paulo, São Carlos

Tita, V., de Medeiros, R., Marques, F.D., Moreno, E.M., 2015, "Effective properties evaluation for smart composite materials with imperfect fiber–matrix adhesion", *Journal of Composites Materials*, Vol. 49(29), pp. 3683-3701.

Totry, E., Molina-Aldareguía, J.M., González, C., et al., 2010, "Effect of fiber, matrix and interphase properties on the in-plane shear deformation of carbon-fiber reinforced composites", *Composites Science and Technology*, Vol. 70, pp. 970–980.

Vajari, D.A., Legarth, B.N., Niordson, C.F., 2013, "Micromechanical modeling of unidirectional composites with uneven interfacial strengths", *European Journal of Mechanics A/Solids*, Vol. 42, pp. 241-250.

Wang, W., Dai, Y., Zhang, C., Gao, X., Zhao, M., 2016, "Micromechanical modeling of fiber-reinforced composites with statistically equivalent random fiber distribution", *Materials*, Vol. 9, pp.624.

Yang, L., Wu, Z., Cao, Y., Yan, Y., 2015, "Micromechanical modelling and simulation of unidirectional fibre-reinforced composite under shear loading", *Journal of Reinforced Plastics and Composites*, Vol. 34(1), pp. 72-83.

Swolfs Y, Verpoest I, Gorbatikh L. A review of input data and modelling assumptions in longitudinal strength models for unidirectional fibre-reinforced composites. *Composite Structures*, Vol.150, pp.153-172.

7. RESPONSIBILITY NOTICE

The authors are the only responsible for the printed material included in this paper.